

Dynamics of equatorial F region irregularities from spaced receiver scintillation observations

A. Bhattacharyya,¹ S. Basu, and K. M. Groves

Air Force Research Laboratory, Space Vehicles Directorate, Hanscom AFB, Massachusetts

C. E. Valladares, and R. Sheehan

Institute for Scientific Research, Boston College, Newton Center, Massachusetts

Abstract. Spaced receiver observations of amplitude scintillations on a 244 MHz signal, at an equatorial station, have been used to study random temporal changes associated with the scintillation-producing irregularities and the variability of their motion. The computed drift of the scintillation pattern shows the presence of velocity structures associated with equatorial bubbles in the early phase of their development. On magnetically quiet days, after 22:00 LT, the estimated drifts fall into a pattern which is close to that of the ambient plasma drift. There is considerable decorrelation between the two signals until 22:00 LT. The power spectra of the most highly correlated scintillations recorded by spaced receivers indicate that the associated irregularities are confined to a thin layer on the bottomside of the equatorial F region. This suggests that the convection pattern associated with bottomside irregularities is stable due to the dominance of ion-neutral collisions over ion inertia.

Introduction

Density structures associated with equatorial ionospheric plasma irregularities which develop after sunset on some nights, are involved in the forward scattering of transionospheric radio waves which propagate through them. Movement of the irregularities across the signal path as well as random changes in them give rise to fluctuations or scintillations in the amplitude and phase of the radio waves recorded by a ground receiver. The temporal structure of weak to moderate amplitude scintillations yields information about the irregularity scale size that contributes the most to amplitude scintillations. This is the Fresnel scale which depends on the signal wavelength and the effective distance, along the signal path, between the receiver and the irregularity layer. Further, presence or absence of Fresnel

oscillations in the power spectrum of the recorded scintillations indicates whether or not the irregularities are confined to a relatively thin layer, of thickness ≤ 100 km. Since the equatorial F region irregularities are highly elongated along the geomagnetic field lines, east-west drift of the scintillation pattern on the ground is measured using receivers spaced in the magnetic east-west direction. In the presence of random variations in the pattern, the signals recorded by two receivers are not perfectly correlated. A parameter, which is a measure of the decorrelation, is also derived from spaced receiver data [Vacchione *et al.*, 1987; Spatz *et al.*, 1988; Bhattacharyya *et al.*, 1989; Basu *et al.*, 1991; Valladares *et al.*, 1996]. Results derived from spaced receiver observations of nighttime equatorial scintillations are described in section 2.

Dual frequency transmissions from Global Positioning System satellites have shown the simultaneous existence of depletions in the total electron content along the signal path due to the presence of equatorial ionospheric bubbles, and amplitude scintillations on L-band signals caused by the density irregularities [Beach and Kintner, 1999; Bhattacharyya *et al.*, 2000]. Plasma bubbles originate in the bottomside equatorial F -region and may extend over several hundred kilometers in altitude. These are seen as highly structured plumes on radar backscatter maps [Woodman and La Hoz, 1976; Tsunoda *et al.*, 1982; Hysell *et al.*, 1994; Hysell, 1999]. Another type of equatorial F -region irregularities are the bottomside irregularities which are confined to a limited altitude extent of 50-100 km on the bottomside of the equatorial F -layer [Valladares *et al.*, 1983; Hysell, 1998]. Scintillations on a VHF signal recorded at an equatorial station without any corresponding observable bubbles in the signal path have been attributed to thin irregularity layers [Dasgupta *et al.*, 1983]. Patches of scintillations which may be attributed to bottom-side equatorial spread F layers are identified in section 3. In section 4, conclusions are drawn regarding the variability of the estimated irregularity drifts and characteristics of bottomside equatorial spread F layers.

Irregularity drift and random velocity

Scintillations observed at Ancon (11.8°S, 77.2°W, dip latitude 0.9°N) are used to study the differences in the

¹Permanently at Indian Institute of Geomagnetism, Mumbai, India.

dynamics of the two different types of equatorial F -region irregularities. The data consists of measurements of amplitude of a 244 MHz signal transmitted from a geostationary satellite, by two ground receivers separated by a distance of 187.8m along the magnetic east-west direction. The sampling frequency of the data is 50 Hz. For 'frozen' irregularities, which drift across the signal path with a constant velocity without undergoing any changes, there is no decorrelation between the signals recorded by the two receivers. Decorrelation due to random changes in the irregularities or their drift velocity is quantified by a parameter V_c , designated the 'random' or 'characteristic' velocity. The average eastward drift speed, V_0 , of the scintillation pattern and V_c are estimated every 82s from the auto- and cross-correlation functions of the two signals. In general, V_0 has contributions from V_E , the eastward drift, as well as V_Z , the vertical drift of the irregularities: $V_0 = V_E - V_Z \tan \theta \sin \phi$,

where θ is the zenith angle and ϕ is the azimuth angle of the signal path measured eastward from the north. For the signal path to Ancon, $\theta \approx 28^\circ$, and $\phi \approx 291^\circ$ such that $V_0 \approx V_E + V_Z/2$.

In Figure 1(a) is shown a mass plot of the eastward drift, V_0 , of the ground scintillation pattern at Ancon during eight magnetically quiet nights in February, 1999. Mass plots of the random velocity computed for the same nights at Ancon are shown in Figure 1(b). Values of V_0 and V_c are computed only when $S_4 > 0.15$, where the S_4 -index is the standard deviation of normalized intensity. This ensures that the drift estimates are not significantly affected by noise. Also if the maximum value of cross-correlation between the two signals falls below 0.5, then the assumptions made, about the form of the space-time correlation function of scintillations, are rendered invalid. Hence computation of V_0 and V_c is not physically meaningful in this case. For these reasons, although equatorial F -region irregularities start to develop shortly after sunset, computed values of V_0 and V_c are available from around 20:00 LT onwards.

Figure 1(a) reveals a great deal of day-to-day variability in the drift of the ground scintillation pattern before 22:00 LT. After 22:00 LT the drifts estimated on different days of the month fall into the same pattern, and therefore may be considered to be representative of the ambient plasma drift. The large variations in the earlier period are attributed to the $\vec{E} \times \vec{B}$ drifts arising from perturbation electric fields associated with equatorial bubbles in the early phase of their development. The mass plot of random velocities also shows large values before 22:00 LT. Results presented in Figure 1(a) indicate that velocity structures associated with perturbation electric fields in the equatorial F region are eroded in a couple of hours after the development of irregularities is initiated, while the density structures associated with scintillation-producing irregularities continue to exist for several hours longer.

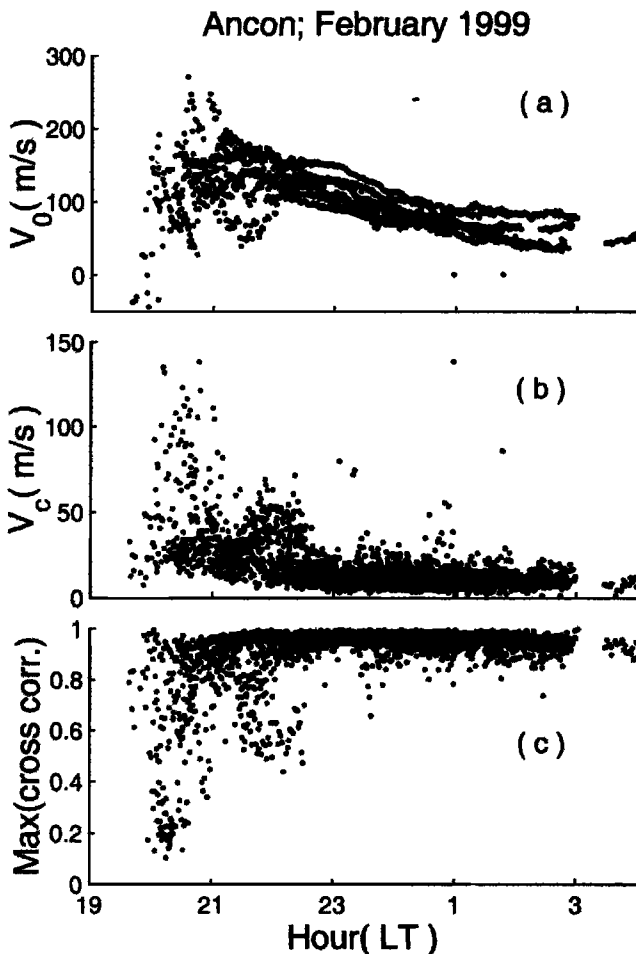


Figure 1. (a) Temporal variation of the eastward drift of the ground scintillation pattern observed at Ancon during eight magnetically quiet nights during February, 1999. (b) Temporal variation of the random velocity derived from spaced receiver scintillation data used to estimate the eastward drifts plotted in (a). (c) Maximum value of cross-correlation between the signals recorded by the spaced receivers as a function of local time.

Bottomside spread F layers

Maximum value of cross-correlation between the two signals for 82s intervals is plotted as a function of local time in Figure 1(c). It is seen that the correlation improves significantly after 22:00 LT which is reflected in smaller values of random velocities illustrated in Fig. 1(b). The most highly correlated intervals of scintillation have temporal characteristics that are different from those found in scintillations occurring at earlier times, as revealed by their respective power spectra. The power spectrum of amplitude scintillations recorded during a 328s period starting at 2008 LT on February 15, 1999, is displayed in Figure 2(a). The power spectrum of highly correlated (maximum cross-correlation = 0.97) amplitude scintillations for a 328s interval during a later period on the same night is displayed in Figure 2(b). Fresnel oscillations are clearly

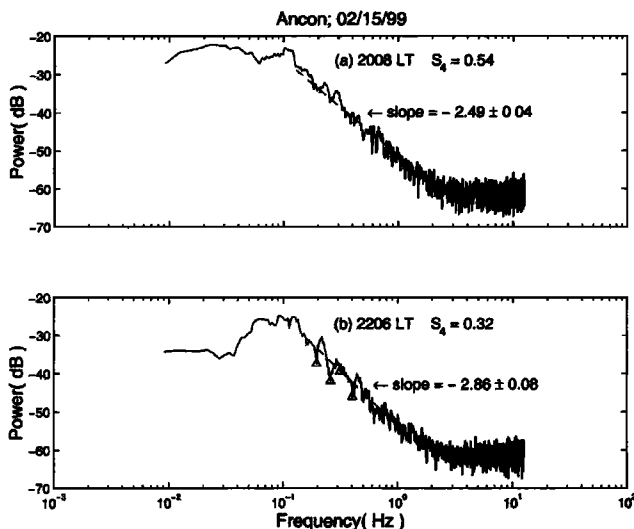


Figure 2. (a) Power spectra of amplitude scintillations recorded during a 5.5 minute period starting at 2008 LT on February 15, 1999. The average values of V_0 and V_c during this period are 115.4 m/s and 40.3 m/s. (b) Power spectra of highly correlated amplitude scintillations recorded during a 5.5 minute period starting at 2206 LT on this night. The first four Fresnel minima are marked by triangles. The average values of V_0 and V_c during this period are 151.9 m/s and 18.6 m/s.

seen in the latter spectrum, where the first four Fresnel minima are marked by triangles. *Basu et al.* [1986] had also reported the presence of Fresnel oscillations in the Fourier spectra of nighttime scintillations which were suggested to be due to bottomside irregularities.

A thin layer of irregularities, producing weak to moderate scintillations, may effectively be represented by a phase changing screen in the path of the incident radio waves. Then, the ratio of the frequencies ν_n and ν_1 corresponding to the n^{th} and first Fresnel minima, respectively, is given by $\nu_n/\nu_1 = \sqrt{n}$. Going beyond the phase screen approximation, it has been demonstrated theoretically [Yeh and Liu, 1982] that for a layer of irregularities of thickness > 100 km, located at a height of 350 km, the Fresnel oscillations are smeared out. Thus, when moderate scintillations are due to irregularities embedded in bubbles which are extended over altitudes of several hundred kilometers, no Fresnel oscillations are expected. This may be the situation for the interval considered in Figure 2(a). The first four Fresnel minima in Figure 2(b) yield the following values for the ratio ν_n/ν_1 : 1.32, 1.61, and 2.1 for $n = 2, 3$, and 4, respectively, which support the conclusion that the irregularity layer during this interval has a thickness less than 100 km. The Fresnel minima are usually well defined, as seen in Figure 2(b). According to theory, $\nu_1 = V_i/(\lambda z_R)^{1/2}$, where V_i is the component of the irregularity zonal drift velocity in a direction normal to the signal path, λ is the signal wavelength, and z_R is the 'reduced' range along the signal path. In terms of the distances z_1 and z_2 along the signal path, between the

phase screen and the receiver, and satellite and phase screen respectively, $z_R = z_1 z_2 / (z_1 + z_2)$. For a geostationary satellite, $z_2 \gg z_1$, such that $z_R \approx z_1$. V_i is related to the estimated eastward drift V_0 of the scintillation pattern on the ground through $V_0 = V_i / \cos \theta$. Thus, estimates of ν_1 from the power spectrum of amplitude scintillations and V_0 from spaced receiver scintillation data allow the determination of z_R . In Figure 2(b), $\nu_1 = 0.195$ Hz, and the average value of V_0 during this interval is 151.9 m/s, which yield an effective slant range of 394 km. Considering the signal path elevation angle at Ancon, the corresponding effective height of the irregularity layer is estimated to be 348 km. This height may correspond to the bottomside of the equatorial *F*-region because of the greater height of the equatorial *F* layer in the early evening hours during solar maximum conditions, and therefore scintillations during this period may be attributed to a bottomside irregularity layer of thickness ≤ 100 km. Although the Fresnel frequency, $\nu_c = V_i / (2\lambda z_R)^{1/2}$, can not be estimated accurately from the broad maximum in the power spectrum of amplitude scintillations, the approximate value of ν_c obtained from Figure 2(a) indicates that with the estimated average value of $V_0 = 115.4$ m/s, the effective slant range for this interval exceeds 1000 km.

Summary

Spaced receiver scintillation observations at Ancon have demonstrated that the motion of the irregularities which cause scintillations is highly variable in the initial phase of irregularity development. These variations follow different patterns on different magnetically quiet days in the same month. This suggests that the estimated drifts should not be considered as representative of the ambient plasma drift until about 22:00 LT. After this hour, the estimated drifts tend to follow the same pattern on different days, and may be compared with zonal drift velocities obtained from incoherent scatter radar observations [Fejer et al., 1981] during non-spread *F* periods.

Scintillations are an integrated effect as far as the whole irregularity layer is concerned, with maximum contribution from the region around the *F*-layer density maximum when the equatorial bubbles extend into the topside. As such, the estimated V_0 may not be attributed to motion of irregularities at a particular location. However, a mass plot of the estimated drifts for a month or a season gives an estimate of the range of variations in the drift that may be expected during that period. In recent computer simulations of the temporal evolution of equatorial *F*-region bubbles, the behavior of a dynamic background plasma and neutral thermospheric components have been taken into account while computing the density and plasma velocities in the region of the bubble [Retterer, 1999]. The extrema of the upward and eastward velocities obtained in such simulations are shown as a function of local time in Fig. 1

of Retterer [1999]. The ranges spanned by the extrema increased rapidly after local sunset, peaked at a certain value and then declined more gradually over a period of one hour, after which the extrema are much closer to the ambient plasma drift. The density structures which represent the bubbles are found to persist long after the velocity structures have been eroded. The mass plot of estimated drifts in Figure 1(a) shows the presence of velocity structures in the initial phase of bubble development. It should be possible to compare this observed feature of the equatorial *F*-region irregularities with results obtained from computer simulations of the development of equatorial bubbles, although at present such simulations are not able to resolve the spatial scales in the density structures which would produce scintillations on a transionospheric UHF signal.

The high degree of correlation found between spaced receiver records of scintillations, which have been shown to arise from thin, bottomside equatorial *F*-region irregularity layers, indicates the absence of random changes in these irregularities or their drift velocities. In a study of chaotic fluid behavior associated with ionospheric turbulence, Huba *et al.* [1985] noted that at altitudes ≤ 400 km, where inertial effects may be negligible compared to ion-neutral collisions, the Rayleigh-Taylor instability would always evolve non-linearly into states with stable convection pattern. The bottomside irregularity layers seem to represent such states. On the other hand, scintillations produced by equatorial *F*-region bubbles prior to 22:00 LT, almost always show a great deal of decorrelation between records obtained at spaced receivers, thus yielding large random velocities. The random changes associated with this type of irregularities may be an indication of chaotic behavior of the plasma expected at higher altitudes according to the theory presented by Huba *et al.* [1985].

Acknowledgments. This work was performed while A. Bhattacharyya held a National Research Council - (AFRL) Senior Research Associateship. The work at the Air Force Research Laboratory was partially supported by AFOSR Task 2310G9.

The Editor would like to thank the reviewer of this manuscript.

References

- Basu, S., *et al.*, Scintillations associated with bottomside sinusoidal irregularities in the equatorial *F*-region, *J. Geophys. Res.*, *91*, 270-276, 1986.
- Basu, S., *et al.*, Zonal irregularity drifts and neutral winds measured near the magnetic equator in Peru, *J. Atmos. Terr. Phys.*, *53*, 743-755, 1991.
- Beach, T. L., and P. M. Kintner, Simultaneous Global Positioning System observations of equatorial scintillations and total electron content fluctuations, *J. Geophys. Res.*, *104*, 22,553-22,565, 1999.
- Bhattacharyya, A., S. J. Franke, and K. C. Yeh, Characteristic velocity of equatorial *F*-region irregularities determined from spaced receiver scintillation data, *J. Geophys. Res.*, *94*, 11,959-11,969, 1989.
- Bhattacharyya, A., T. L. Beach, S. Basu, and P. M. Kintner, Nighttime equatorial ionosphere: GPS scintillations and differential carrier phase fluctuations, *Radio Sci.*, *35* 209-224, 2000.
- Dasgupta, A. *et al.*, VHF amplitude scintillations and associated electron content depletions as observed at Arequipa, Peru, *J. Atmos. Terr. Phys.*, *45*, 15-26, 1983.
- Fejer, B. G. *et al.*, *F* region east-west drifts at Jicamarca, *J. Geophys. Res.*, *86*, 215-218, 1981.
- Huba, J. D., A. B. Hassam, I. B. Schwartz, and M. J. Keiskinen, Ionospheric turbulence: Interchange instabilities and chaotic fluid behavior, *Geophys. Res. Lett.*, *12*, 65-68, 1985.
- Hysell, D. L., M. C. Kelley, W. E. Swartz, and D. T. Farley, VHF radar and rocket observations of equatorial spread *F* on Kwajalein, *J. Geophys. Res.*, *99*, 15,065-15,085, 1994.
- Hysell, D. L., Imaging coherent scatter radar studies of bottomside equatorial spread *F*, *J. Atmos. Sol. Terr. Phys.*, *60*, 1109-1122, 1998.
- Hysell, D. L., Imaging coherent backscatter radar studies of equatorial spread *F*, *J. Atmos. Sol. Terr. Phys.*, *61*, 701-716, 1999.
- Retterer, J. M., Theoretical model for fast equatorial bubbles, *Proceedings of Ionospheric Effects Symposium*, pp 688-691, Alexandria, Virg., 1999.
- Spatz, D. E., S. J. Franke, and K. C. Yeh, Analysis and interpretation of spaced receiver scintillation data recorded at an equatorial station, *Radio Sci.*, *23*, 347-361, 1988.
- Tsunoda, R. T., R. C. Livingston, J. P. McClure, and W. B. Hanson, Equatorial plasma bubbles: Vertically elongated wedges from the bottomside *F*-layer, *J. Geophys. Res.*, *87*, 9171-9180, 1982.
- Vacchione, J. D., S. J. Franke, and K. C. Yeh, A new analysis technique for estimating zonal irregularity drifts and variability in the equatorial *F* region using spaced receiver scintillation data, *Radio Sci.*, *22*, 745-756, 1987.
- Valladares, C. E., *et al.*, The multi-instrumented studies of equatorial thermosphere aeronomy scintillation system: climatology of zonal drifts, *J. Geophys. Res.*, *101*, 26,839-26,850, 1996.
- Valladares, C. E., W. B. Hanson, J. P. McClure, and B. L. Cragin, Bottomside sinusoidal irregularities in the equatorial *F* region, *J. Geophys. Res.*, *88*, 8025-8042, 1983.
- Woodman, R. F., and C. La Hoz, Radar observations of *F*-region equatorial irregularities, *J. Geophys. Res.*, *81*, 5447-5466, 1976.
- Yeh, K. C., and C. H. Liu, Radio wave scintillations in the ionosphere, *Proc. IEEE*, *70*, 324-360, 1982.
- S. Basu, A. Bhattacharyya, and K. M. Groves, Air Force Research Laboratory, Space Vehicles Directorate, (AFRL/VSB1), 29 Randolph Road, Hanscom AFB, MA 01731-3010. (e-mail: Santimay.Basu@hanscom.af.mil; archana@iig.iigm.res.in; Keith.Groves@hanscom.af.mil)
- R. Sheehan, and C. E. Valladares, Institute for Scientific Research, Boston College, 885 Centre Street, Newton, MA 02159. (e-mail: sheehan@plh.af.mil; ceasar@dl5000.bc.edu)

(Received September 1, 2000; accepted October 2, 2000.)